Transmission Expansion Planning via Unconventional High Surge Impedance Loading (HSIL) Lines

Bhuban Dhamala *Student Member*, *IEEE*, and Mona Ghassemi, *Senior Member*, *IEEE*Zero Emission, Realization of Optimized Energy Systems (ZEROES) Laboratory

Department of Electrical and Computer Engineering, The University of Texas at Dallas, Richardson, TX, USA bhuban.dhamala@utdallas.edu, mona.ghassemi@utdallas.edu

Abstract—Transmission expansion planning (TEP) plays a vital role in ensuring the reliable and efficient operation of power systems, especially with the growing demand for electricity and the integration of renewable energy sources. This paper focuses on applying unconventional high surge impedance loading (HSIL) lines in transmission expansion planning and compares their outcomes with conventional line-based transmission expansion planning. Starting with a 17 bus- 500 kV power system connected by a conventional transmission line, the objective is to connect a new load located in a new bus, bus #18, to the existing 17-bus power system via two approaches: using conventional lines and incorporating unconventional HSIL lines. By comparing the number of lines required for the conventional and unconventional approaches, maintaining almost identical conductor volume per circuit, the effectiveness of unconventional HSIL lines in TEP is evaluated where using only two unconventional HSIL lines is sufficient to connect 1000 MW load demand at bus 18 while three lines are required when using the conventional design.

Index Terms—Transmission expansion planning, power systems, unconventional high surge impedance loading lines.

I. INTRODUCTION

The modern power industry has been restructured into a horizontally integrated open market system consisting of independent generation, transmission, and distribution sectors. This restructuring has brought about substantial alterations in both supply and demand sides. On the supply side, traditional large synchronous generators have given way to lighter generators and variable renewable energy resources. Similarly, highly modernized efforts can be witnessed on the demand side-a growing number of distributed variable energy resources, efficient energy storage technology, a shift to electronic converters, the concept of demand response and demand side management, and energy-saving solutions in buildings, industrial equipment, and consumer devices. However, no significant changes have been made in the hardware of transmission sector, the highways transporting electric energy within power systems, over the decade-long history of the large-scale interconnected power industry.

In the realm of electrical power transmission, the utilization of overhead three-phase transmission has served as a

prominent and influential method in the past, and its prevalence is expected to persist in the future. While underground presents an alternative option for power transmission, the cost of underground cables is three to ten times the cost of overhead lines [1, 2], with higher ratios for higher voltage. Furthermore, underground AC cables present technical challenges that limit their transmission length due to their high charging current.

As industries expand, and reliance on electricity becomes more prominent, demand for electric power continues to rise. Due to the increasing commitment of international societies to low carbon emissions and with exceptional advancements in technology, the integration of large-scale renewable energy sources is, nowadays, highly increased. Renewable energy generation often occurs in remote or resource-rich areas, which may be distant from the demand centers and existing transmission infrastructure. The transfer of renewable energies from these remote areas to power grids requires cost-effective TEP scenarios. Moreover, increasing the extent of critical loads typically requires a reliable and uninterruptible power supply to avoid any disruptions or failures that could have severe consequences. This motivates the power industry to enhance grid resilience and reliability. Transmission expansion facilitates the efficient delivery of electricity from generation sources to consumption centers, ensuring the growing power demandis met adequately. Therefore, transmission expansion planning is a crucial process in the development and improvement of power systems for reliable, efficient, and sustainable electricity transmission, and the integration of large-scale renewable sources, such as wind and solar, is a significant driver for transmission expansion planning.

Conventional transmission lines have served as reliable means of energy transmission for many years. Fulfilling the escalating demand for reliable and efficient energy from distant sources in modern societies necessitates a substantial increase in the capacity of transmission lines. However, conventional transmission lines face technical, economic as well as environmental limitations that hinder the significant expansion of power transmission capacity. Limitations such as voltage drop, voltage stability, transient and dynamic instability, and fault current tolerance impose restrictions on the amount of power that can be transmitted [3]. Upgrading the existing

This work was supported in part by the National Science Foundation (NSF) under Award #2306098.

system and acquiring the right-of-way for new transmission lines entail substantial costs. Moreover, expanding transmission corridors for new lines adversely affects natural habitats, causing environmental degradation. Therefore, there is a pressing need for more advanced transmission technologies to address these challenges. High Surge Impedance Loading (HSIL) lines may present a compelling solution, offering significant advantages over conventional lines in terms of power transfer capability.

A comprehensive review of HSIL lines, evaluating the technical gaps and outlining future research requirements, has been conducted in [4]. A detailed study on compact transmission lines with different conductor bundles in terms of surge impedance loading (SIL), electrostatic and electromagnetic unbalance factors, the contribution of each phase charge to field intensity on the ground surface, and conductor surface gradient has been analyzed in [5]. Reference [3] shares the valuable experience gained from implementing HSIL lines in Brazil. This study has also identified two key geometric factors: compacting the phases and expanding the conductors' bundle, as effective methods for enhancing the SIL. In [6], conventional HSIL lines were studied, these lines featured symmetrically positioned subconductors on the circles across all phases. This study revealed a significant correlation between surge impedance loading and the uniformity of the electric field.

This paper presents a study focusing on the expansion of high-voltage power systems to efficiently supply a load in a new location, prioritizing proximity within the transmission network. The primary objective of this research is to assess the effectiveness and performance of two distinct transmission line technologies: conventional transmission lines and unconventional high surge impedance loading (HSIL) lines on transmission expansion planning and aim to expand the power system network to successfully meet the load demand, while simultaneously establishing cost-effective planning scenarios that result in a substantial saving. Different aspects of unconventional HSIL lines were studied [7-14], and in this paper, our focus is on the role that they play in TEP studies.

II. PROPOSED BASE CASE POWER SYSTEM NETWORK

A. Power Network Topology

The proposed test power network to demonstrate the extensive analysis of transmission expansion planning has 17buses, with 8 generators. Fig. 1 shows the single-line diagram of the test power system considered. The transmission line lengths for individual lines are presented in Table I. The system voltage is considered 500 kV. Generation and load information for 17 buses are indicated in Table II. All loads have a 0.9 lagging power factor which is taken as the usual power factor assumption for TEP studies.

B. Conventional Transmission Line Configuration

Fig. 2 shows the configuration of the 500 kV conventional transmission line presented in [5] with 4 subconductors in the bundle. Each dot represents a subconductor and its location. This line configuration with the Macaw conductor has been selected as the conventional line in this paper. Specific data for

this conductor and line parameters of this configuration are shown in Table III, the case named "Conven."

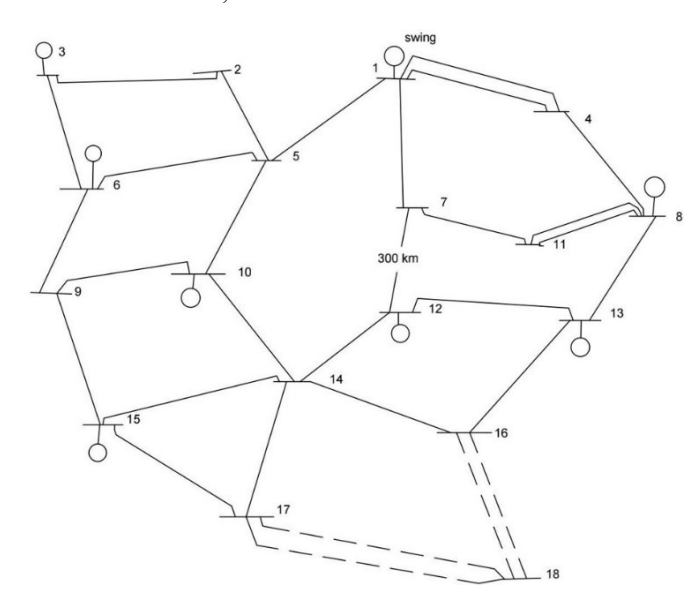


Fig. 1. The 17-bus network considered in this paper as the base power system for the TEP study.

TABLE I
EXISTING TRANSMISSION LINES IN 17-BUS NETWORK

Line	Length (km)	Line	Length (km)
1-4	474.19	8-11(2 circuit)	349.09
1-5	430.91	8-13	360.00
1-7	370.91	9-10	447.27
2-3	485.45	9-15	398.18
2-5	294.55	10-14	392.73
3-6	349.55	12-13	561.29
4-8	416.13	12-14	348.38
5-6	519.00	13-16	490.91
5-10	376.36	14-15	572.73
6-9	316.36	14-16	499.09
7-11	387.09	14-17	403.64
7-12	300.00	15-17	561.29

TABLE II
LOAD AND GENERATION DATA OF 17-BUS TEST SYSTEM

Bus (Type)	V (p.u)	P (MW)	Q (MVar)
Bus1 (Slack)	1.05	-	-
Bus2 (PQ)	-	$P_{L} = 900$	$Q_L = 435.9$
Bus3 (PV)	1.03	$P_{\rm g} = 2000, P_{\rm L} = 1000$	$Q_L = 484.3$
Bus4 (PQ)	-	$P_{L} = 1250$	$Q_L = 505.6$
Bus5 (PQ)	-	$P_{L} = 950$	$Q_L = 460.1$
Bus6 (PV)	1.01	$P_g = 1700, P_L = 500$	$Q_L = 242.2$
Bus7 (PQ)	-	$P_{L} = 1400$	$Q_L = 678.1$
Bus8 (PV)	1.04	$P_g = 1600, P_L = 1000$	$Q_L = 678.1$
Bus9 (PQ)	-	$P_{L} = 1000$	$Q_L = 484.3$
Bus10 (PV)	1.03	$P_g = 2000, P_L = 1019$	$Q_L = 493.1$
Bus11 (PQ)	-	$P_{L} = 1000$	$Q_L = 484.3$
Bus12 (PV)	1.02	$P_g = 2200, P_L = 800$	$Q_L = 387.5$
Bus13 (PV)	1.02	$P_g = 2300, P_L = 650$	$Q_L = 314.8$
Bus14 (PQ)	-	$P_{L} = 1100$	$Q_{L} = 532.8$
Bus15 (PV)	1.00	$P_g = 2000, P_L = 1800$	$Q_L = 871.1$
Bus16 (PQ)	-	$P_{L} = 950$	$Q_L = 460.1$
Bus17 (PQ)	-	$P_{L} = 800$	$Q_{L} = 387.5$

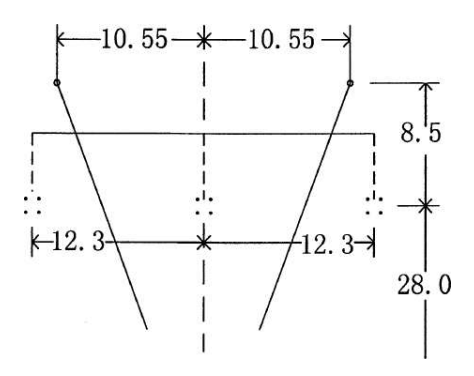


Fig. 2. The conventional line considered for the test system shown in Fig. 1.

TABLE III
LINE PARAMETERS FOR MACAW CONDUCTOR USED FOR CONVENTIONAL
AND UNCONVENTIONAL LINES

case	Conductor type	L (mH/km)	C (nF/km)	R (Ω/km)
Conven.	Macaw, φ=1.055 In	0.878	12.975	0.0228
Unconven.	Tailorbird, φ=0.823 In	0.593	19.009	0.0180

C. Power Flow Analysis for the Proposed Base Case

AC power flow analysis problem is formulated as:

$$I = Y_{bus}V \tag{1}$$

$$P_i + jQ_i = V_i I_i^* \tag{2}$$

$$P_{i} = |V_{i}| \sum_{k=1}^{n} |V_{k}| |Y_{ik}| \cos(\delta_{i} - \delta_{i} - \theta_{ik})$$
 (3)

$$Q_i = |V_i| \sum_{k=1}^n |V_k| |Y_{ik}| \sin(\delta_i - \delta_i - \theta_{ik})$$
 (4)

where δ_i and $|V_i|$ are the phase angle and magnitude of the voltage at bus i, n is the number of buses in the network, Y_{ik} are the elements of Y_{bus} that is the admittance matrix, θ_{ik} is the angle of Y_{ik} . P_i and Q_i are the injected real and reactive power into the bus i.

Considered constraints for the power flow analysis are:

$$0.95 \le |V_i| \le 1.05 \ p. u.$$
 (5)

$$-0.3P_{gi} \le Q_{gi} \le 0.6P_{gi} \tag{6}$$

$$S_{ik} \le S_{ik}^{max} \tag{7}$$

Eq. (5) represents the voltage constraint in the power system during normal operating and Eq. (6) is the reactive power generation limit for each generating unit, P_{gi} , presented in Table II. Eq. (7) is the apparent power flow limit in the transmission line connecting bus i and k. Maximum power flow, S_{ik}^{max} , is determined by the thermal limit of the mentioned line.

Using four Macaw conductors per bundle, the thermal limit

of the line is $3\times(500 \text{ kV})\times(4\times0.870 \text{ kA})=3014 \text{ MVA}$. 80% of the thermal limit, 2400 MVA, is considered the line rating, S_{ik}^{max} .

Newton Raphson method is used to solve the power flow problem of Eqs. (1)–(4) with constraint from Eqs. (5)–(7) for the 17-bus power system under normal condition with the generation and load data presented in Table II. The results of the load flow analysis are presented in Table IV.

TABLE IV
LOAD FLOW ANALYSIS RESULTS FOR 17-BUS SYSTEMS UNDER
NORMAL OPERATING CONDITION

Bus #	V (p.u)	δ (deg.)	Pg (MW)	Qg (MVar)
1	1.05	0.00	2590.8	-654.6
2	0.980	-22.175	0.0	0.0
3	1.03	5.581	2000.0	193.0
4	1.04	-18.648	0.0	0.0
5	1.04	-18.443	0.0	0.0
6	1.01	-0.828	1700.0	-344.9
7	0.959	-24.066	0.0	0.0
8	1.04	-14.143	1600.0	-259.1
9	0.998	-24.811	0.0	0.0
10	1.04	-16.225	2000.0	-243.1
11	1.021	-26.053	0.0	0.0
12	1.02	-9.386	2200.0	-90.7
13	1.03	-0.807	2300.0	-269.3
14	1.048	-34.039	0.0	0.0
15	1.00	-31.543	2000.0	-130.4
16	0.974	-36.392	0.0	0.0
17	1.041	-46.701	0.0	0.0

The load flow analysis result shown in Table IV indicates that the per unit voltage in all buses, reactive power generation by all generating units, and power flow in all lines are within the defined range indicated in Eqs. (5)–(7).

III. TRANSMISSION EXPANSION PLANNING (TEP)

Consider the transmission expansion planning problem of supplying a load of 1000 MW with a power factor of 0.9 lagging at a new bus, referred to as bus #18. The nearest buses available to connect this new load to the 17-bus power system are bus #16 and bus #17, located at distances of 463.64 km and 475.73 km, respectively. Assume that the required generation to meet this new load can be provided through the slack bus, bus #1.

A. TEP Using the Conventional Line

Using well-established technology of conventional lines for transmission line expansion may be a convenient option. The three connecting options are analyzed as possible expansion options: two lines from bus #16 to bus #18, two lines from bus #17 to #18, and a line from bus #16 to bus #18 and a line from bus #17 to #bus 18. The load flow solution cannot be converged in any of the three TEP scenarios mentioned above. Therefore we consider a three-circuit TEP scenario, three lines between bus #16 and #18. This scenario works of course with adding more reactive power compensation to ensure the voltage level at all buses remains within the specified limit, Eq. (5). The summarized power flow results for this three-conventional-lines case from bus #16 to bus #18 are shown in Table V.

TABLE V
POWER FLOW ANALYSIS RESULTS WITH THREE CONVENTIONAL LINES
FROM BUS #16 TO BUS #18 BUS
UNDER NORMAL OPERATING CONDITION

Bus #	V (p.u)	δ (deg.)	Pg (MW)	Qg (MVar)
1	1.050	0.000	3816.6	-45.4
2	0.986	-37.223	0.0	0.0
3	1.030	-11.302	2000.0	166.8
4	1.013	-25.292	0.0	0.0
5	1.039	-32.615	0.0	0.0
6	1.010	-18.80	1700.0	-245.2
7	0.958	-37.931	0.0	0.0
8	1.040	-30.702	1600.0	-280.4
9	0.977	-46.948	0.0	0.0
10	1.030	-37.741	2000.0	50.3
11	1.022	-41.799	0.0	0.0
12	1.020	-31.491	2200.0	123.2
13	1.030	-27.643	2300.0	243.8
14	0.983	-64.453	0.0	0.0
15	1.000	-58.458	2000.0	99.9
16	0.966	-91.856	0.0	0.0
17	1.004	-76.683	0.0	0.0
18	1.005	-104.34	0.0	0.0

This power flow result satisfies all the requirements for normal operating condition. The voltage level for each bus and the reactive power generation limit for all generating units meet Eqs. (5) and (6). The maximum loadings of lines are 64% for line 13-16, 55% for line 1-7, and 50% for 12-14, well below the rating mentioned in Section II.C. However, this TEP scenario requires another line and two additional bays as compared to using the two-line TEP scenarios. These additional requirements make this TEP scenario more costly. An intriguing question is whether the unconventional arrangement of conductor bundles can effectively meet this demand, utilizing two-line TEP scenarios for example from bus #18 to bus #16 or #17. We will answer this question in the following sections.

B. TEP Using the Unconventional HSIL Line

To design an unconventional HSIL line, a modification is made to the conventional design constraint arranging the subconductors symmetrically in bundles in all phases. Instead, subconductors can be positioned anywhere in space. By altering the spatial positioning of subconductors, it becomes feasible to enhance the loading capacity of the transmission line, manifesting through an increase in surge impedance loading. To optimize the surge impedance loading, the precise arrangement of subconductors in unconventional HSIL lines can be determined while meeting the overhead line electrical design constraints outlined in Eqs. (8) to (11).

$$E^{max} < E_{nr} \tag{8}$$

$$D_{ab}^{p2p} > D^{p2p.min} \ a, b \in \{1, 2, 3\} \ and \ a \neq b$$
 (9)

$$D_{min}^{p2g} > D_{pr}^{p2g} \tag{10}$$

Symmetry of configuration must be maintained (11)

The first constraint, Eq. (8), states that the maximum electric field on the surface of the subconductors, E^{max} , cannot exceed a permissible value, E_{pr} , which is determined by the corona onset gradient. The second constraint, Eq. (9), indicates that the distance between subconductors of different phases must be greater than a minimum value. The third constraint, Eq. (10), indicates that the minimum height of subconductors to the ground must be above a minimum permissible height, D_{pr}^{p2g} . The final constraint ensures symmetrical mechanical loading of the tower. To find the conductor position, the initial step involves compacting the configurations to a level where the maximum electric field intensity on subconductors approaches its upper limit. Then, the capacitance of phases is equalized so that the phases' maximum electric field is maximized. This approach enables the attainment of the maximum surge impedance loading while considering the trade-off with the maximum electric field intensity on subconductors. Following this, the compactness of the line is adjusted again to adhere to the constraint related to the surface electric field. Finally, the optimal position of each subconductor is determined based on the considerations and adjustments.

Considerations involved to design HSIL lines for this analysis are $E_{pr}=20\,$ kV/cm, $D^{p2p.min}=6.7\,$ m, and $D^{p2g}_{pr}=24\,$ m. The maximum height allowed for subconductors is set at 32 m in order to avoid high towers, which would increase the cost. Fig. 3 shows the geometry of the restructured high power density line or unconventional HSIL line where the Tailorbird conductor having an outer diameter of 0.823 inches, mentioned in Table III, has been selected in an 8-subconductor bundle format per phase. Using Tailorbird conductor with a smaller outer diameter than Macaw conductor, the unconventional HSIL line with eight Tailorbird conductors per bundle has a smaller total aluminum cross-section than the conventional line with four Macaw conductors per bundle, so the unconventional HSIL line will not be more expensive than the conventional line.

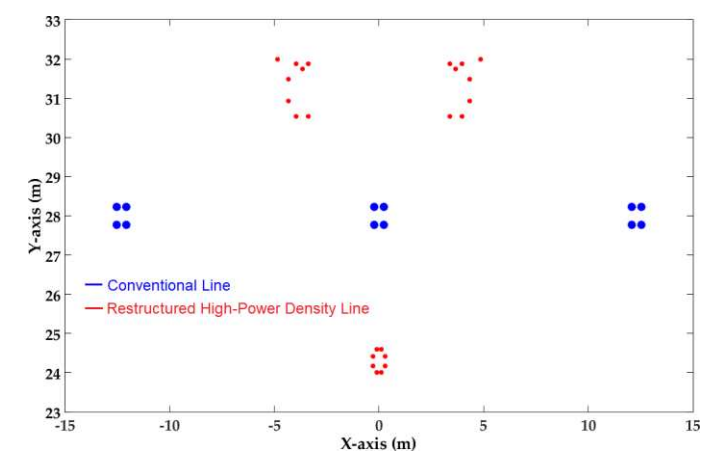


Fig. 3. Arrangement phase and subconductors for the conventional line and unconventional HSIL line.

Conductor specifications and line parameters of the unconventional line configuration are shown in Table III. The

maximum electric field on the surface of the subconductors of the unconventional HSIL line is 19.73 kV/cm and its surge impedance loading (SIL) is 1414.68 MW. The total width of the line is 9.904 m. This unconventional HSIL line increases SIL by 1.43 times and decreases tower width by 2.53, resulting in 3.6 times more power density than the conventional line.

A TEP study has been performed using this unconventional HSIL line designed above to supply the load at bus #18. The analysis shows that instead of using three conventional lines from bus #16 to bus #18 as mentioned in Section III.A and Table V, only two unconventional HSIL lines from bus #16 to bus #18 can supply 1000 MW load with a 0.9 lagging power factor at bus #18. The load flow results for this case are shown in Table VI. The maximum loadings of lines are 64% for line 13-16, 60% for line 1-4, and 50% for line 1-7, well below the mentioned rating in section II.C.

TABLE VI
POWER FLOW RESULTS FOR THE TEP SCENARIO WITH TWO
UNCONVENTIONAL HSIL LINES FROM BUS #16 TO BUS #18
UNDER NORMAL CONDITION

Bus #	V (p.u)	δ (deg.)	Pg (MW)	Qg (MVar)
1	1.050	0.000	3822.4	-34.8
2	0.984	-37.400	0.0	0.0
3	1.030	-11.445	2000.0	169.6
4	1.013	-25.301	0.0	0.0
5	1.038	-32.773	0.0	0.0
6	1.010	-18.946	1700.0	-239.5
7	0.957	-38.057	0.0	0.0
8	1.040	-30.723	1600.0	-279.3
9	0.976	-47.129	0.0	0.0
10	1.030	-37.983	2000.0	18.9
11	1.022	-41.857	0.0	0.0
12	1.020	-31.710	2200.0	90.4
13	1.030	-27.614	2300.0	271.1
14	0.997	-64.509	0.0	0.0
15	1.000	-58.586	2000.0	60.4
16	0.953	-92.397	0.0	0.0
17	1.018	-76.529	0.0	0.0
18	0.993	-105.463	0.0	0.0

As seen from Table VI, the voltage amplitude at all buses and reactive power generation for all generating units meet Eqs. (5) and (6). Furthermore, the lines with maximum loadings are also well below the thermal rating of the line, meeting Eq. (7).

Other aspects of this work, using a revised version of the test system meeting all single contingencies in addition to the normal condition [15, 16] are presented in our other papers [17, 18]. Among the difficulties of designing HSIL lines, live line working may be challenging due to the interaction of maintenance personnel and those compact lines with unconventional bundle arrangements especially in freezing conditions [19-23].

IV. CONCLUSION

In this paper, an analysis of the transmission expansion planning (TEP) problem using a novel transmission line concept that we call unconventional HSIL lines was introduced. Studies were carried out on a 17-bus 500 kV power system as a base case. The goal was to cost-effectively connect

a new load of 1000 MW with a 0.9 lagging power factor located on a new bus, bus #18, to the existing 17-bus power grid. AC load flow studies showed that we need at least three conventional lines to connect bus #18 to the existing transmission network meeting both voltage amplitude and line loading limits while it is possible to do this via two unconventional HSIL lines. In the unconventional HSIL, the conductor type was selected to make the cost comparable to the conventional line. Therefore, the TEP problem considered in this paper with the unconventional HSIL line designed in this paper can achieve remarkable savings regarding a line and two bays less than the same TEP problem using the conventional line.

REFERENCES

- [1] F. Kiessling, P. Nefzger, and U. Kaintzyk, Overhead power Lines, Planning Design, Construction, Berlin, Germany: Springer, 2003.
- [2] Commonwealth of Virginia, Joint Legislative Audit and Review Commission, Evaluation of Underground Electric Transmission Lines in Virginia, House Document No. 87, 2006.
- [3] C. K. Arruda, L. A. M. C. Domingues, A. L. Esteves dos Reis, F. M. Absi Salas, and J. C. Salari, "The optimization of transmission lines in Brazil: Proven experience and recent developments in research and development," *IEEE Power and Energy Mag.*, vol. 18, no. 2, pp. 31-42, Mar.-Apr. 2020.
- [4] M. Ghassemi, "High surge impedance loading (HSIL) lines: A review identifying opportunities, challenges, and future research needs," *IEEE Trans. Power Del.*, vol. 34, no. 5, pp. 1909-1924, Oct. 2019.
- [5] H. Wei-Gang, "Study on conductor configuration of 500 kV Chang-Fang compact line," *IEEE Trans. on Power Del.*, vol. 18, no. 3, pp. 1002-1008, Jul. 2003.
- [6] R. G. Olsen and C. Zhuang, "The spatial distribution of electric field as a unifying idea in transmission line design," *IEEE Trans. Power Del.*, vol. 34, no. 3, pp. 919-928, Jun. 2019.
- [7] M. Abedin Khan and M. Ghassemi, "A new unusual bundle and phase arrangement for transmission line to achieve higher natural power," *IEEE North American Power Symp. (NAPS)*, Asheville, NC, USA, 2023.
- [8] M. Abedin Khan and M. Ghassemi, "Calculation of corona loss for unconventional high surge impedance loading (HSIL) transmission lines," *IEEE North American Power Symp. (NAPS)*, Asheville, NC, USA, 2023.
- [9] M. Abedin Khan and M. Ghassemi, "A new method for calculating electric field intensity on subconductors in unconventional high voltage, high power density transmission lines," *IEEE Conf. Electrical Insul. Dielectric Phenomena (CEIDP)*, East Rutherford, NJ, USA, 2023.
- [10] M. Abedin Khan and M. Ghassemi, "Calculation of audible noise and radio interference for unconventional high surge impedance loading (HSIL) transmission lines," *IEEE Conf. Electrical Insul. Dielectric Phenomena (CEIDP)*, East Rutherford, NJ, USA, 2023.
- [11] J. Hernández, J. Segundo-Ramirez, P. Gomez, M. Borghei, and M. Ghassemi, "Statistical switching overvoltage studies of optimized unconventional high surge impedance loading lines via numerical Laplace transform," *IEEE Trans. Power Del.*, vol. 36, no. 4, pp. 2145–2153, 2021.
- [12] M. Borghei and M. Ghassemi, "Geometrically optimized phase configurations and sub-conductors in the bundle for power transmission efficiency," *IEEE Electrical Insul. Conf. (EIC)*, Calgary, Canada, 2019, pp. 295–298.
- [13] M. Borghei and M. Ghassemi, "Future transmission lines with increased loadability through geometrical optimized phase configurations and subconductors in the bundle," *IEEE Innovative Smart Grid Technol. Conf.* (ISGT), Washington, DC, USA, 2020.
- [14] J. Hernández, J. Segundo, P. Gomez, M. Borghei, and M. Ghassemi, "Electromagnetic transient performance of optimally designed high surge impedance loading lines," *IEEE Power & Energy Society General Meeting (PESGM)*, Montreal, QC, Canada, 2020.
- [15] B. Dhamala and M. Ghassemi, "A test system for transmission expansion planning studies meeting the operation requirements under normal condition as well as all single contingencies," *IEEE North American Power Symp. (NAPS)*, Asheville, NC, USA, 2023.

- [16] B. Dhamala and M. Ghassemi, "A test system for transmission expansion planning studies for both normal condition and all single contingencies," *IEEE Open Access Journal of Power and Energy*, submitted for publication, 2023.
- [17] B. Dhamala and M. Ghassemi, "Unconventional high surge impedance loading (HSIL) lines and transmission expansion planning," *IEEE North American Power Symp. (NAPS)*, Asheville, NC, USA, 2023.
- [18] B. Porkar, M. Ghassemi, and M. Abedin Khan, "Transmission expansion planning (TEP)-based unconventional high surge impedance loading (HSIL) line design concept," *IEEE North American Power Symp. (NAPS)*, Asheville, NC, USA, 2023.
- [19] M. Ghassemi, M. Farzaneh, and W. A. Chisholm, "Three-dimensional FEM electrical field calculation for FRP hot stick during EHV live-line work," *IEEE Trans. Dielectr. Electr. Insul.*, vol. 21, no. 6, pp. 2531–2540, Dec. 2014.
- [20] M. Ghassemi, M. Farzaneh, and W. A. Chisholm, "A coupled computational fluid dynamics and heat transfer model for accurate estimation of temperature increase of an ice-covered FRP live-line tool," *IEEE Trans. Dielectr. Electr. Insul.*, vol. 21, no. 6, pp. 2628–2633, Dec. 2014.
- [21] M. Ghassemi and M. Farzaneh, "Coupled computational fluid dynamics and heat transfer modeling of the effects of wind speed and direction on temperature increase of an ice-covered FRP live-line tool," *IEEE Trans. Power Del.*, vol. 30, no. 5, pp. 2268–2275, Oct. 2015.
- [22] M. Ghassemi and M. Farzaneh, "Effects of tower, phase conductors and shield wires on electrical field around FRP hot stick during live-line work," *IEEE Trans. Dielectr. Electr. Insul.*, vol. 22, no. 6, pp. 3413–3420, Dec. 2015.
- [23] M. Ghassemi and M. Farzaneh, "Calculation of minimum approach distances for tools for live working under freezing conditions," *IEEE Trans. Dielectr. Electr. Insul.*, vol. 23, no. 2, pp. 987–994, Apr. 2016.